SANS Study of the Structural Phases of Magnetically Alignable Lanthanide-Doped Phospholipid Mixtures

Mu-Ping Nieh,*,†,‡ Charles J. Glinka,† and Susan Krueger†

Materials Science and Engineering Laboratory, National Institute of Standards and Technology, Gaithersburg, Maryland 20899, and Department of Materials Science, Pennsylvania State University, University Park, Pennsylvania 16802

R. Scott Prosser

Department of Chemistry and Liquid Crystal Institute, Kent State University, Kent, Ohio 44242

John Katsaras

National Research Council, Steacie Institute for Molecular Sciences, Neutron Program for Material Research, Chalk River Laboratories, Chalk River, Ontario, Canada

Received November 9, 2000. In Final Form: February 7, 2001

The structural phases of magnetically alignable lipid mixtures were investigated as a function of temperature and lipid concentration using small-angle neutron scattering (SANS). Two systems were examined: (a) an aqueous mixture of DMPC (dimyristoyl phosphatidylcholine) and DHPC (dihexanoyl phosphatidylcholine) lipids doped with Tm^{3+} ions resulting in the positive alignment of the system with the applied magnetic field and (b) the above aqueous Tm^{3+} doped lipid mixture containing a negatively charged lipid, DMPG (dimyristoylphosphatidylglycerol). For both systems, three different scattering patterns were observed corresponding to distinct structural phases at specific temperatures and lipid concentrations. At 45 °C and a lipid concentration of >0.05 g/mL, the high-viscosity liquid crystalline phase was found to be a perforated and possibly undulating lamellar phase consistent with NMR results. Upon dilution (<0.05 g/mL) at the same temperature (45 °C), the perforated lamellar phase transformed into a unilamellar vesicular phase, in which the bilayers may also be perforated. Below about 25 °C, the viscosity decreases considerably and the scattering data suggest that the lamellae present at higher temperatures break up into smaller entities characterized by the bicellar morphology proposed previously for the nondoped system. The structural dimensions of the vesicular and bicellar phases have been determined as a function of lipid concentrations from the SANS data. In the lamellar phase, the influence of Tm^{3+} ions and DMPG on bilayer structure (e.g., lamellar repeat spacing, bilayer rigidity, and magnetic alignment) were also investigated.

Introduction

To understand the biophysics of membrane associated peptides and membrane proteins, it is useful to employ an aligned model system. In the case of solid-state NMR or various spectroscopic techniques, which benefit from the oriented transition dipole moments, the aligned spectra often have higher sensitivity and are easier to interpret than powder spectra.[1] Magnetically aligned membranes are also useful in low-angle X-ray and neutron diffraction studies. If the phase consists of a regularly spaced lamellar structure, the position and the "sharpness" of the Bragg peaks can be used to evaluate the membrane structure and alignment.

Magnetically aligned lipid bilayers are readily formed from mixtures of a phospholipid, such as dimyristoyl phosphatidylcholine (DMPC), with a shorter chain amphiphile, such as dihexanoyl phosphatidylcholine (DHPC). Under appropriate conditions, these mixtures are reported to result in bilayered micelles, or so-called "bicelles" (i.e., molar ratio of DMPC/DHPC between 2.5 and 5 at temperatures between 37 and 45 °C and lipid concentration, c_{lp}, between 0.05 and 0.35 g/mL).[2−4] The morphology of the aggregates is presumed to be a disk whose diameter is expected to range from a few hundred to nearly 1000 Å, depending on the ratio of DMPC/DHPC.[2,3] The short-chain DHPC is believed to be principally sequestered to a rim, which coats the hydrophobic edges of the DMPC-rich bilayer. This mixture was previously believed to form a nematic liquid crystalline phase, that aligns in a magnetic field, such that the average bilayer normal, **n**, is perpendicular to the applied field, **B** (so-called negative alignment). This magnetically alignable membrane system is typically stable under varying pH and salt concentrations[4] and is generally stable upon incorporation of modest amounts of membrane associated peptides.[5−8] Therefore, bicelles have become an enormously popular alignable model membrane in solid-state NMR studies of membrane peptides.

* To whom correspondence should be addressed. Mu-Ping Nieh, Materials Science and Engineering Laboratory, National Institute of Standards and Technology, Gaithersburg, MD 20899.

† National Institute of Standards and Technology.

‡ Pennsylvania State University.

(1) Sanders, C. R.; Hare, B. J.; Howard, K. P.; Prestegard, J. H. *Prog. Nucl. Magn. Reson. Spectrosc.* **1994**, *26*, 421.

(2) Sanders, C. R.; Schwonek, J. P. *Biochemistry* **1992**, *31*, 8898.

(3) Vold, R. R.; Prosser, R. S. *J. Magn. Reson., Ser. B* **1996**, *113*, 267.

(4) Sanders, C. R.; Prosser, R. S. *Ways & Means* **1998**, *6*, 1227.

(5) Sanders, C. R.; Landis, G. C. *J. Am. Chem. Soc.* **1994**, *116*, 647.

(6) Sanders, C. R.; Landis, G. C. *Biochemistry* **1995**, *34*, 4030.

(7) Vold, R. R.; Prosser, R. S.; Deese, A. J. *J. Biomol. NMR* **1997**, *9*, 329.

(8) Struppe, J.; Komives, E. A.; Taylor, S. S.; Vold, R. R. *Biochemistry* **1998**, *37*, 15523.

10.1021/la001567w CCC: $20.00
Published on Web 03/28/2001

Unfortunately, bicelles are not ideal for the study of larger membrane proteins. Unless the studied protein undergoes fast axially symmetric motion around the bilayer normal, the resultant NMR spectrum is a so-called cylindrical powder pattern. Thus, the practical molecular weight limit for solid-state NMR studies of membrane peptides, possessing multiple labels, in bicelles, is probably a few thousand daltons. One solution to this problem is to dope the liquid crystal with appropriate lanthanide ions (usually Tm^{3+} or Yb^{3+}). The lanthanide ions bind to the lipid phosphate groups, thereby conferring a significant positive magnetic susceptibility anisotropy to the membrane, such that $\mathbf{n}||\mathbf{B}$.[9−12] In this case, assuming that the membrane protein can be reconstituted, there is no restriction to the size of the protein for solid-state NMR studies. If scattering techniques are employed, the decomposition of structure information at $\mathbf{Q}||\mathbf{n}$ (out-of-plane) and $\mathbf{Q}\perp\mathbf{n}$ (in-plane) is easier with this lanthanide-doped membrane.

The ^2H NMR result of a Tm^{3+}-doped lipid mixture at high T (45 °C) and $c_{lp} = 0.25$ g/mL by Prosser et al. showed a better resolved spectrum, compared to the non-Tm^{3+}-doped mixture at the same conditions. The authors proposed that the lanthanide-doped mixture was a well-ordered smectic, rather than a nematic, phase.[11] Although they suggested a bilayer morphology resembling that of slices of Swiss cheese formed by the aggregation of the bicelles, the exact morphology of the system remained uncertain.

We have investigated two lanthanide-doped bilayer systems, DMPC/DHPC/Tm^{3+} and DMPC/DMPG/DHPC/Tm^{3+} (with molar ratios of 3.2/1.0/0.043 and 3.2/0.21/1.0/0.043, respectively), as a function of T and c_{lp} in the presence and absence of a magnetic field. The negatively charged lipid, DMPG (dimyristoylphosphatidylglycerol), is useful for stabilizing bilayer systems.[10,13] Furthermore, negatively charged lipids (on the order of 10%) are common constituents of biological membranes. Using small-angle neutron scattering (SANS) measurements on these two samples, we have addressed the following issues: (a) the global structure of the lanthanide-doped bilayer system as a function of temperature and water content, (b) the effect of Tm^{3+} ions on the bilayer structure and alignment, and (c) the effect of DMPG on the properties of the bilayer system.

Experimental Method

Sample Preparation. Phospholipids (DMPC, DHPC, and DMPG) were purchased from Avanti Polar Lipids (Birmingham, AL) and used without further purification. (The identification of any commercial product or trade name does not imply endorsement or recommendation by the National Institute of Standards and Technology.) Thulium chloride hexahydrate (99.99%) was obtained from Aldrich Chemicals (Milwaukee, WI). The samples consisted of DMPC/DHPC/Tm^{3+} in a molar ratio of 3.2/1.0/0.043 (denoted as PC) or DMPC/DMPG/DHPC/Tm^{3+} in a molar ratio of 3.2/0.21/1.0/0.043 (denoted as PC+PG). Tm^{3+} possesses the largest positive magnetic anisotropy of the lanthanide series and is therefore the ideal choice for alignment in the presence of an applied magnetic field. Note that the Tm^{3+} concentration in the above samples was only 10% of that employed in a previous neutron diffraction study.[9]

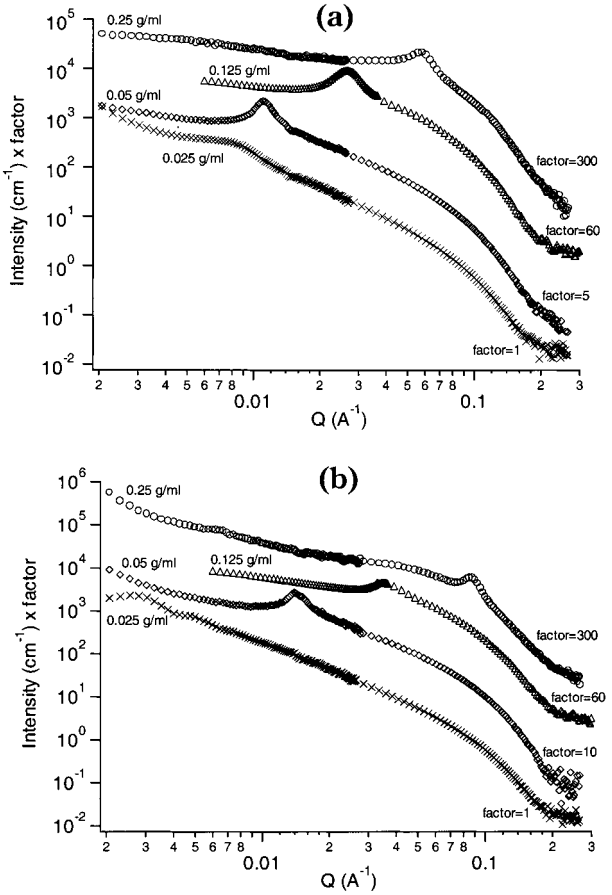

Figure 1. The circularly integrated intensities of (a) PC and (b) PC+PG samples as a function of Q. The data are labeled by the total lipid concentration c_{lp} of each sample. The scattering curves have been scaled by the arbitrary factors indicated to better distinguish the curves. At $c_{lp} = 0.025$ g/mL, the scattering data reflect the coexistence of lamellae and unilamellar vesicles.

For the dilution experiments, the lipid concentration, c_{lp}, varied from 0.00125 to 0.25 g/mL in 99.9% deuterium oxide (D_2O, Cambridge Isotope Co.). For each series (e.g., PC or PC+PG), the sample was prepared at the highest c_{lp} (0.25 g/mL) value, as described previously.[2,10] These concentrated samples were diluted with D_2O to obtain samples of lower c_{lp}.

For contrast variation experiments, lipid mixtures having a fixed c_{lp} (0.25 g/mL) were prepared in solvent mixtures of D_2O and deionized water. Samples with D_2O percentages of 100%, 60%, 40%, 20%, 15%, 10%, and 0% were produced in order to probe the internal structure of the lipid bilayers.

Instrument and Data Reduction. Experiments were conducted using the NG3 and NG7 30m SANS instruments at the NIST Center for Neutron Research located at the National Institute of Standards and Technology (Gaithersburg, MD).[14] For most experiments, a neutron wavelength (λ) of 5 Å was used, covering a Q-range 0.002 Å^{-1} < Q < 0.3 Å^{-1} where Q is defined as $4\pi/\lambda \sin\theta/2$, where θ is the scattering angle between the incident and the scattered neutron beams. For the lower portion of the Q-range, 0.002 Å^{-1} < Q < 0.005 Å^{-1}, a set of biconcave lenses was placed before the sample to focus the beam onto the two-dimensional position-sensitive detector, which was 15 m from the sample.[15] For this configuration, λ of 8.44 Å was used instead of 5 Å.

For the magnetic alignment measurements, an electromagnet capable of ~2 T was employed. A sample stage was designed to orient the sample in the magnetic field to access both out-of-plane and in-plane structures. The sample holder was temper-

(9) Katsaras, J.; Donaberger, R. L.; Swainson, I. P.; Tennant, D. C.; Tun, Z.; Vold, R. R.; Prosser, R. S. *Phys. Rev. Lett.* **1997**, *78*, 899.
(10) Prosser, R. S.; Volkov, V. B.; Shiyanovskaya, I. V. *Biochem. Cell Biol.* **1998**, *76*, 443. Prosser, R. S.; Volkov, V. B.; Shiyanovskaya, I. V. *Biophys. J.* **1998**, *75*, 2163.
(11) Prosser, R. S.; Hwang, J. S.; Vold, R. R. *Biophys. J.* **1998**, *74*, 2405.
(12) Katsaras, J. *Physica B* **1998**, *241*, 1178.
(13) Losonczi, J. A.; Prestegard, J. H. *J. Biomol. NMR* **1998**, *12*, 447.
(14) Glinka, C. J.; Barker, J. G.; Hammouda, B.; Krueger, S.; Moyer, J. J.; Orts, W. J. *J. Appl. Crystallogr.* **1998**, *31*, 430.
(15) Choi, S. M.; Barker, J. G.; Glinka, C. J.; Cheng, Y. T.; Gammel, P. L. *J. Appl. Crystallogr.* **2000**, *33*, 793.

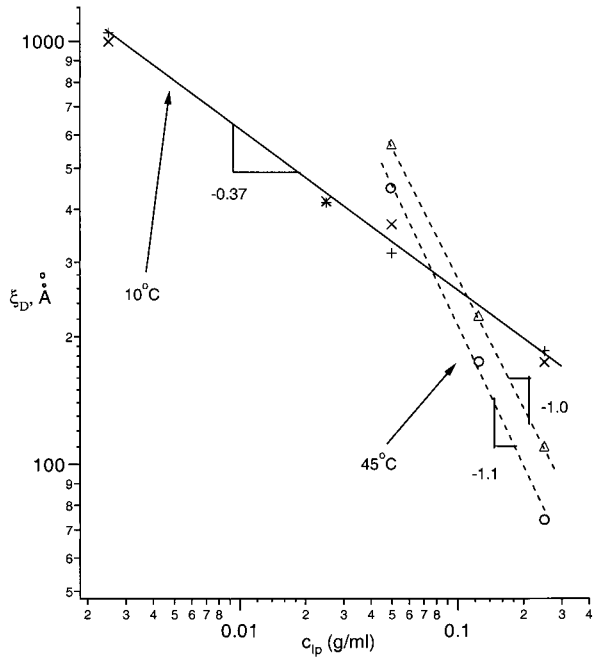

Figure 2. The interlamellar spacing, ξ_D, as a function of total lipid concentration, c_{lp}. The PC and PC+PG series are denoted by Δ and ○, respectively, at $T = 45$ °C and by + and ×, respectively, at 10 °C. The dashed lines are the linear least-squares (LLS) fits, where the slopes are -1.0 ± 0.2 for the PC and -1.1 ± 0.2 for the PC+PG mixture at 45 °C. Similarly, the solid line represents a LLS fit for 10 °C, and the slope is found to be -0.37 ± 0.5 for both series of mixtures.

ature controlled using a circulating water bath. Samples were placed into rectangular quartz cells with a path length of 1 mm and a window size of 8 mm × 13 mm. Both the quartz cells and the samples were maintained at a temperature of ~10 °C during the cell-loading process. At this temperature, the sample adopts a phase with low viscosity.

The 2-D raw data were corrected for ambient background and empty cell scattering and put on an absolute scale (cross section per unit volume) by a procedure that estimates the neutron flux on the sample.[14] The zero-field data were then circularly averaged to yield the 1-D intensity distribution or $I(Q)$. The incoherent scattering from hydrogen was approximated from the high Q intensity plateau and subtracted from the corresponding reduced data.

Results

A. Absence of an Applied Magnetic Field. *I. High Temperature (45 °C) and c_{lp} between 0.05 and 0.25 g/mL.* At 45 °C and $c_{lp} = 0.25$ g/mL, the 2-D SANS data from the PC and PC+PG samples exhibited isotropic diffraction rings. These patterns were circularly integrated and are presented as a function of Q in Figure 1a and b. The scattering intensity of both series shows a peak at a position, Q_{peak}, corresponding to an interparticle spacing, ξ_D, approximately equal to $2\pi/Q_{peak}$. Upon dilution (0.05 g/mL < c_{lp} < 0.25 g/mL), Q_{peak} shifts toward lower values of Q indicative of a continuous increase in ξ_D. Moreover, for $c_{lp} > 0.05$ g/mL the interparticle spacing, ξ_D, varies as $c_{lp}^{-1.0\pm0.2}$ and $c_{lp}^{-1.1\pm0.2}$ for the PC and PC+PG samples, respectively, as shown in Figure 2. This scaling is indicative of 1-D swelling, as would be the case for two-dimensional structures such as bilayer sheets, which change little upon dilution.[11]

Contrast variation experiments can provide more specific information on the internal structure of the bilayer as the scattering length density (SLD) of the solvent, $\rho_{solvent}$, approaches the SLD of the lipid's hydrophobic acyl chains, $\rho_{hydrophobic}$. Figure 3a shows that the total scattering

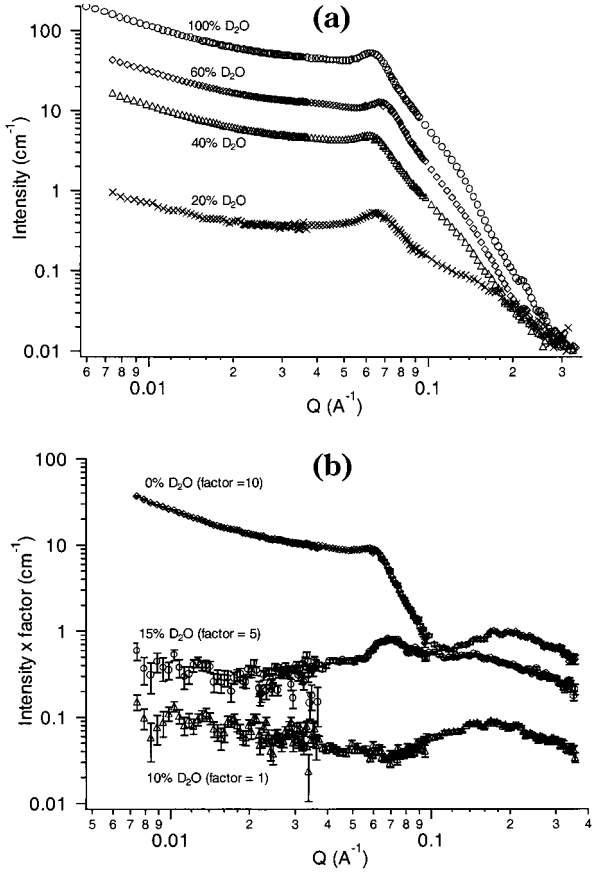

Figure 3. SANS contrast-variation experiment results for a PC+PG mixture at $T = 45$ °C and $c_{lp} = 0.25$ g/mL. The data are labeled by the D_2O composition in the solvents. (a) At higher D_2O composition (> 20%), away from the null contrast condition, the decrease of the peak intensity indicates that $\rho_{solvent}$ is approaching ρ_{lipid}. (b) As $\rho_{solvent}$ approaches ρ_{lipid}, the scattering curves reveal the internal structure of the lamellae. To better distinguish the data, the scattering curves have been scaled up by the arbitrary factors indicated beside the data.

intensity of a PC+PG mixture at a c_{lp} of 0.25 g/mL decreased as $\rho_{solvent}$ approached the average SLD of the lipids, ρ_{lp}, though the shape of scattering pattern remained relatively constant. A ξ_D of 98 ± 5 Å was determined from the peak position. This ξ_D value is in contrast to that obtained from the data presented in Figure 1b where ξ_D was found to be ~74 Å. This may be due to a slightly different amount of the DMPG added into the sample in each preparation. For D_2O compositions less than 20%, the scattering patterns were dramatically different as shown in Figure 3b. The peak associated with ξ_D vanished at 10% D_2O, indicating that $\rho_{solvent} \approx \rho_{lipid}$. This composition is consistent with the calculated null contrast value of 12% D_2O. Nevertheless, a perfect null contrast condition ($\rho_{solvent} = \rho_{lipid}$) is not expected because $\rho_{solvent}$ cannot simultaneously match both $\rho_{hydrophilic}$ and $\rho_{hydrophobic}$ (the SLD for the hydrophilic and hydrophobic components of the bilayer, respectively). For the samples whose D_2O composition was between 0% and 20%, a peak in the vicinity of $Q = 0.18 \pm 0.03$ Å^{-1} appears, which is directly related to $d_{philic-philic}$, the center distance from one side of hydrophilic layer to the other across the bilayer. The $d_{philic-philic}$ is equal to ($t_{bilayer} - t$), where $t_{bilayer}$ and t are the total bilayer and hydrophilic layer thicknesses, respectively. The hydrophilic layer thickness was estimated to

Table 1. Total Lipid Volume Fractions for the Samples Measured, ϕ_{lp}, the Lamellar Spacing, ξ_D, the Volume Fraction for Ideal Lamellae, $\phi_{calc} = \xi_D/t_{bilayer}$, Where $t_{bilayer}$ Is the Bilayer Thickness, and the Ratios ϕ_{lp}/ϕ_{calc}

	PC			PC+PG		
ϕ_{lp} ($\sim c_{lp}$)	0.25	0.125	0.05	0.25	0.125	0.05
ξ_D (Å)	110 ± 5	224 ± 10	571 ± 20	74 ± 4	174 ± 10	449 ± 20
ϕ_{calc} (ideal lamellae)	0.39 ± 0.05	0.19 ± 0.02	0.075 ± 0.01	0.58 ± 0.05	0.25 ± 0.02	0.095 ± 0.01
ϕ_{lp}/ϕ_{calc}	0.64 ± 0.1	0.65 ± 0.1	0.66 ± 0.1	0.43 ± 0.06	0.50 ± 0.06	0.52 ± 0.06

be 8 Å.[16,17] By use of the approximate formula, $2\pi/Q_{peak} = d_{philic-philic}$, ($t_{bilayer} - t$) can be estimated to be 35 ± 2 Å resulting in $t_{bilayer} = 43 \pm 2$ Å.

For well-dispersed and perfectly flat lamellae composed of uniformly distributed lipids, the lipid volume fraction can be calculated from the simple expression $\phi_{calc} = t_{bilayer}/\xi_D$. The ϕ_{calc} values based on such "ideal lamellae" have been estimated from the SANS data and are listed in Table 1. Usually the lamellae are flexible and contain undulations[18−22] or ripples[23,24] on the surface, and therefore the experimentally prepared ϕ_{lp} would be expected to be larger than ϕ_{calc}.[18,19] However, in the present case ϕ_{calc} values are larger than ϕ_{lp}. This could indicate the coexistence of lipid-rich and solvent-rich regions in the sample or/and nonuniform bilayers, perhaps resulting from perforation or toroidal defects created by DHPC domains in the lamellae.

Two major differences are observed between the SANS data from PC mixtures and that from PC+PG mixtures. For the PC+PG mixture, the scattering intensity at low Q values is higher, resembling the scattering from larger aggregates, and ξ_D is smaller. This would be consistent with the formation of lipid-rich and solvent-rich domains in the PC+PG samples. A smaller ξ_D would also be expected upon the addition of DMPG, because Coulomb repulsion from the Tm^{3+} ions between the bilayers is reduced. As for the PC series, ξ_D increases less than 6% (from 110 to 116 Å) as the Tm^{3+} ion concentration is increased 10-fold, implying that the bilayer sheets are already well dispersed in the solution.[9] However, for ϕ_{lp} ($\sim c_{lp}$) = 25% and $t_{bilayer} = 43$ Å, as discussed above, we would expect a ξ_D of ~170 Å for the ideal lamellae. This value is still 1.5 times the ξ_D obtained in the high Tm^{3+} ion case. Thus, the PC and PC+PG systems were not ideal lamellae and a perforated structure, as illustrated in Figure 4, cannot be ruled out.

The perforated lamellar phase can be distinguished from the well-known multilamellar vesicular structure for pure DMPC solutions by the continuous swelling behavior for DMPC/DHPC mixtures upon decreasing c_{lp}. The formation of these perforated lamellae is expected to arise from short-chain DHPC concentrating on the edge of the lamellar sheets as well as the rim of the pores, thus reducing the penalty incurred by the curvature energy.

We attempted to model this phase as a stack of N infinitely extended and flat (including $N \rightarrow \infty$) perforated bilayers with no in-plane correlation between the perforations. This model agrees with the experimental data in the high-Q regime beyond the peak position; however, in the low-Q regime the calculated scattering intensity follows a Q^{-2} dependence and overestimates the experimental data. This may be due to the interference effects resulting from the undulations of the lamellae, which were not taken into account in our flat lamellar model.

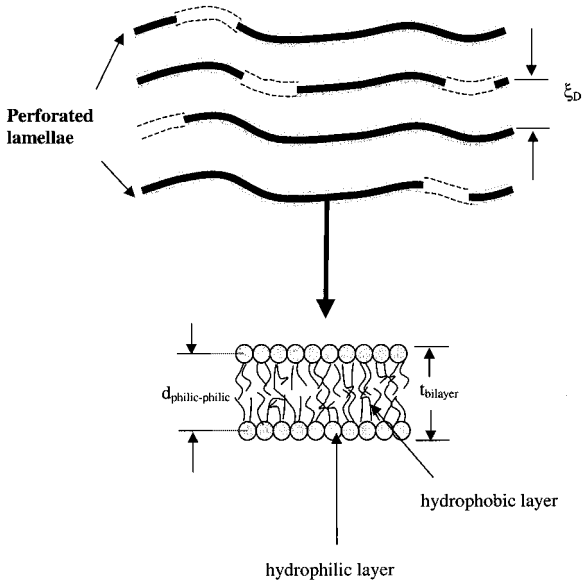

Figure 4. Schematic of the perforated lamellar model. The dotted regions represent pores on the bilayer surface, and the blow-up sketch shows the inner structure of the lamellae.

II. High Temperature (45 °C) and 0.00125 g/mL < c_{lp} < 0.025 g/mL. As we decreased c_{lp} to 0.025 g/mL, the scattering peak shifted to such a small Q value that it was no longer observable (Figure 1a,b). A weak oscillation along the scattering curve, which is unexpected for a sheetlike phase at such T and c_{lp}, was observed, indicative of a new morphology coexisting with the bilayer-sheet phase. Upon further dilution, down to $c_{lp} = 0.00125$ g/mL, the scattering from this new phase shown in Figure 5, which cannot be described using the previous model, is more characteristic of isolated globular particles. This scattering is consistent with a vesicular phase model.

As shown in Figure 6a, the vesicular model is described by a spherical shell filled with and surrounded by the aqueous solution. The outer and inner radii are defined as R_o and R_i, respectively. The particle size distribution is represented by the Schulz distribution, $f(r)$, with the polydispersity, p, defined as $\sigma/\langle R_o \rangle$, where σ^2 is the variance of R_o and $\langle R_o \rangle$ represents the average R_o. Theoretically, there are variations in the SLD across the shell. Because $\rho_{solvent}$ is much higher than both $\rho_{hydrophilic}$ and $\rho_{hydrophobic}$, the scattering is not very sensitive to variations in the SLD within the shell. Hence, we used a single, average ρ_{lipid} for the SLD of the shell in our model calculations. The form factor of a unilamellar vesicle, $P_{vesicle}(Q)$, can be written as

$$P_{vesicle}(Q) = \frac{1}{V_{vesicle}} \int_0^\infty f(r)\, A_o^2(Qr)\, dr \qquad (1)$$

(16) Buldt, G.; Gally, H. U.; Seelig, J.; Zaccai, G. *J. Mol. Biol.* **1979**, *134*, 673.
(17) Nagle, J. F.; Zhang, R.; Tristram-Nagle, S.; Sun, W.; Petrache, H. I.; Suter, R. M. *Biophys. J.* **1996**, *70*, 1419.
(18) Helfrich, W. *J. Phys.* (*Paris*) **1985**, *46*, 1263.
(19) Skouri, M.; Marignan, J.; Appell, J.; Porte, G. *J. Phys. II* **1991**, *1*, 1121.
(20) Peliti, L.; Leibler, S. *Phys. Rev. Lett.* **1985**, *54*, 1690.
(21) Cevc, G. *Biochim. Biophys. Acta* **1991**, *1062*, 59.
(22) Walz, J. Y.; Ruckenstein, E. *J. Phys. Chem. B* **1999**, *103*, 7461.
(23) Lubensky, T. C.; Mackintosh, F. C. *Phys. Rev. Lett.* **1993**, *71*, 1565.
(24) Sengupta, K.; Raghunathan, V. A.; Katsaras, J. *Europhys. Lett.* **2000**, *49*, 722.

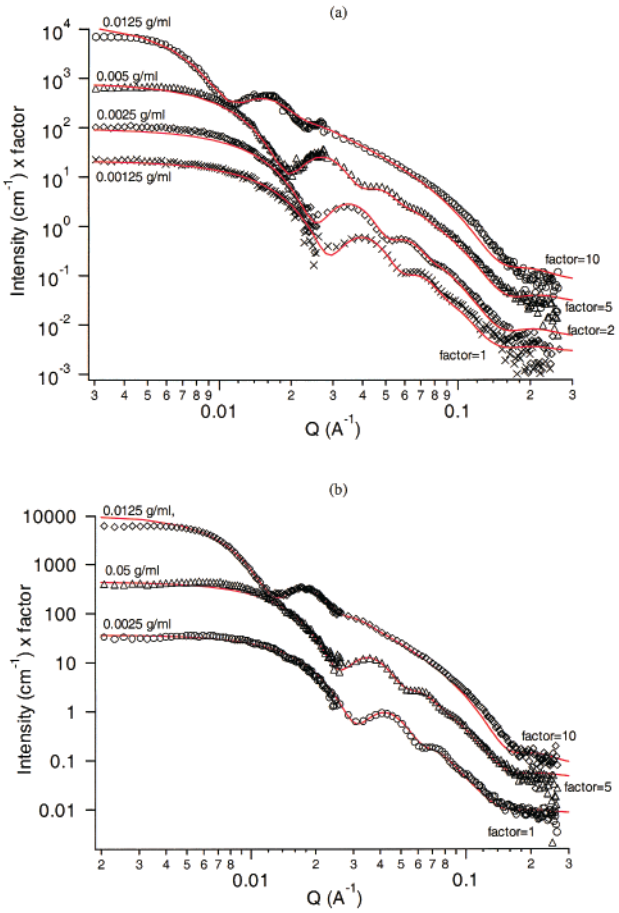

Figure 5. SANS results for (a) PC and (b) PC+PG series mixtures at 45 °C and low total lipid concentration, c_{lp} (0.00125 g/mL ≤ c_{lp} ≤ 0.0125 g/mL), as a function of the scattering vector, Q. The data are labeled by the c_{lp}. The solid curves are the best-fit results using a vesicular model. The model parameters are listed in Table 2. To better distinguish the curves, the scattering intensities have been scaled by the arbitrary factors illustrated beside the data.

where $V_{vesicle}$ is the total volume of a unilamellar vesicle and

$$A_o(Qr) = \frac{4\pi(\rho_{lipid} - \rho_{solvent})}{Q^3}\left[\left(\sin Q\frac{R_i}{R_o}r - \sin Qr\right) - Qr\left(\frac{R_i}{R_o}\cos Q\frac{R_i}{R_o}r - \cos Qr\right)\right]$$

$$f(r) = \frac{(p^{-2/p^2})\left(\frac{r}{\langle R_o\rangle}\right)^{(1-p^2)/p^2} e^{-r/p^2\langle R_o\rangle}}{\langle R_o\rangle\Gamma(1/p^2)}$$

$\Gamma(1/p^2)$ is the Gamma function, where a reasonable value for p is in the range of 0−1. The detailed derivation of the scattering function for this vesicular model has been carried out by Hayter.[25]

Neglecting any interparticle interference, the scattering data were fit with $\phi_{lp,fit}P_{vesicle}(Q)$. The $\rho_{solvent}$ for D_2O was calculated to be 6.38×10^{-6} Å^{-2} and was fixed during the fitting procedure. Our best fits are presented as solid curves in Figure 5. The excellent agreement between the experimental data and the fits strongly supports our proposed model. Only a slight deviation between the experimental and fitted data at $Q < 0.01$ Å^{-1} is found, possibly because of interparticle interference effects, which become less noticeable as we decrease c_{lp}. In Table 2, we present the fitted parameters for the vesicular model of both the PC and PC+PG series. The consistency of the fitted ρ_{lipid} (3.2×10^{-7} Å^{-2}) with the calculated ρ_{lipid} (3.3×10^{-7} Å^{-2}) further supports the proposed vesicular model. The value of $(R_o - R_i) = 36 \pm 3$ Å is relatively constant and close to the center-to-center distance between two hydrophilic layers in the bilayer, $d_{philic-philic}$, obtained in the high-c_{lp} lamellar phase (∼35 Å), indicating the vesicles are unilamellar. R_i (or R_o) is c_{lp}-dependent in both series, though less so in the PC+PG series as compared with the PC. Nevertheless, the morphology and the critical c_{lp} (∼0.025 g/mL) for this phase transition are the same for both series, suggesting the addition of DMPG does not alter the basic morphology for this phase.

(25) Hayter, J. B. In *Physics of Amphiphilies*; Degiorgio, V., Corti, M., Eds.; Amsterdam, 1985; p 59.

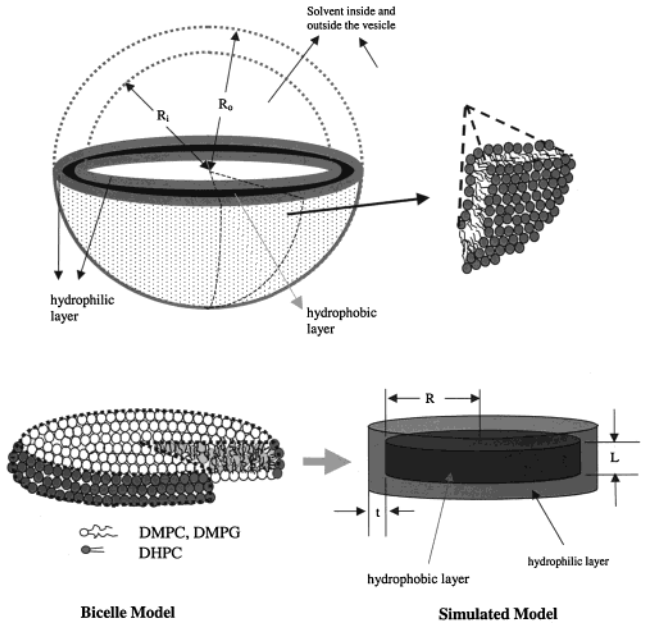

Figure 6. (a) The proposed unilamellar vesicular model with solvent inside and outside the vesicle; the blow-up shows a slice of the detailed structure of the unilamellar vesicles. (b) The proposed bicelle model by Vold and Prosser (ref 3). The short-chain lipids (DHPC) are at the rim, and the long-chain lipids (DMPC or DMPG) are at the top and bottom surfaces. The simplified model is a core−shell disk with the core (hydrophobic layer) having a radius R, the core thickness L, and the hydrophilic shell thickness t.

III. Low Temperature (10 °C). Figure 7 illustrates the scattering results from the PC and PC+PG series of mixtures at 10 °C. A broad scattering peak corresponding to ξ_D is observed, which shifts toward lower Q values upon dilution. Except for the shifting "Bragg" peak, the pattern of scattering is similar for all the c_{lp} values studied (0.0025−0.25 g/mL), implying that the morphology of the system is independent of lipid concentration. Unlike the data at 45 °C, ξ_D, at equivalent values of c_{lp}, was practically identical for both the PC and PC+PG mixtures although the two systems have drastically different charge densities. Moreover, ξ_D varied as $c_{lp}^{-0.37\pm0.05}$ (Figure 2), which is nearly indistinguishable from the $-1/3$ scaling exponent indicative of swelling in 3-D. The unfailing result of this scaling law throughout the whole c_{lp} studied suggested that neither fusion nor aggregation of the particles occurred in the solution. For this reason, the morphology was believed to be unchanged with c_{lp} at the same temperature, 10 °C. The 3-D swelling, combined with the fact that the visually

Table 2. Structural Parameters of the Vesicular Phase at 45 °C with ϕ_{lp} Varying from 1.25% to 0.125%[a]

	PC				PC+PG		
$\phi_{lp,act}$ (%)	1.25	0.5	0.25	0.125	1.25	0.5	0.25
$\phi_{lp,fit}$ (%)	2.2 ± 0.2	0.64 ± 0.05	0.25 ± 0.02	0.13 ± 0.02	2.2 ± 0.2	0.51 ± 0.05	0.25 ± 0.02
R_o(Å)	257 ± 20	166 ± 15	133 ± 12	119 ± 12	233 ± 20	128 ± 12	110 ± 10
$*R_i$[b] (Å)	220 ± 20	130 ± 15	96 ± 10	81 ± 7	197 ± 20	93 ± 8	73 ± 5
p	0.2 ± 0.03	0.14 ± 0.03	0.13 ± 0.03	0.13 ± 0.03	0.17 ± 0.03	0.16 ± 0.03	0.16 ± 0.03
$*\rho_{lipid}$[b] (Å^{-2})				$(3.2 \pm 0.5) \times 10^{-7}$			

[a] The tabulated values are the best-fit results for $\phi_{lp,fit}$, R_o, R_i, p, and ρ_{lipid}, representing the fitted total lipid volume fraction, outer radius, inner radius, polydispersity, and the average SLD of the lipid, respectively. [b] The asterisk represents parameters that were constrained within the reasonable ranges according to literature reports or calculation.

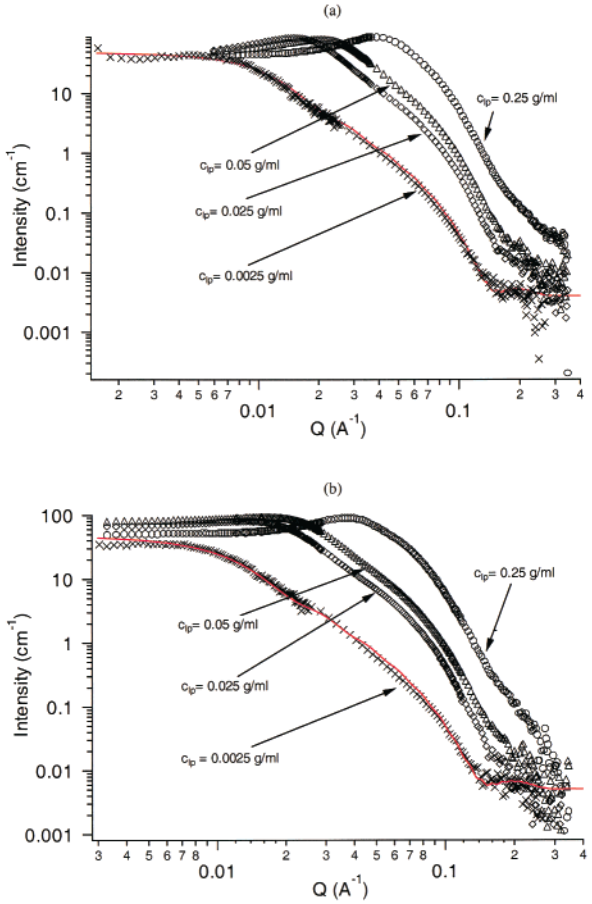

Figure 7. SANS results for (a) PC and (b) PC+PG series mixtures at 10 °C as a function of the scattering vector, Q. The data are labeled by the c_{lp}. Only the $c_{lp} = 0.0025$ g/mL scattering data could be fit (solid curve) using the core−shell−disk model.

transparent system has low viscosity at this temperature,[2−4] suggests that the morphology is that of small particles, which are highly mobile in the solvent. The NMR results for this phase also suggest a randomly oriented isotropic morphology.[9]

The first attempt to characterize the scattering pattern with a core−shell−sphere model, representing a spherical micellar structure, failed to fit the data. The structure of this phase then was characterized using a simplified version of the bicelle model as proposed in the literature for the nondoped lipid system at temperatures above 35 °C and high c_{lp} (>0.05 g/mL).[3,4] The proposed model in Figure 6b is represented by disks with flat, rather than curved, edges for simplification. The outer hydrophilic shell and the inner hydrophobic core are composed of the phosphatidylcholine headgroups and fatty acid chains, respectively. The dimension R represents the hydrophobic core radius, and L and t describe the thicknesses of the core and shell, respectively. The form factor of such a core−shell disk, $P_{disk}(Q)$, after orientational averaging can be expressed as

Table 3. Structural Parameters for the Bicellar Disk Model Used to Fit the Lowest Concentration, $\phi_{lp} = 0.0025$ g/mL, Data at 10 °C[a]

	PC	PC+PG
R (Å)	196 ± 20	189 ± 20
$*t$[b] (Å)	8.4 ± 2	7 ± 2
L (Å)	34 ± 2	35 ± 2
$*\rho_{hydrophilic}$[b] (Å^{-2})	$(3.2 \pm 0.5) \times 10^{-6}$	$(3.3 \pm 0.5) \times 10^{-6}$

[a] The tabulated values are the best-fit results for R, t, L, and $\rho_{hydrophilic}$, which represent the radius of the core, the thickness of the shell, the thickness of the core, and the SLD of the shell, respectively (Figure 6b). [b] The asterisk represents parameters that were constrained within the reasonable ranges according to literature reports or calculation.

$$P_{disk}(Q) = \int_0^{\pi/2} \frac{g^2(Q,\alpha)}{V_{lipid}} \sin\alpha \, d\alpha$$

where

$$g(Q,\alpha) = 2(\rho_{hydrophobic} - \rho_{hydrophilic})V_{hydrophobic} \times \frac{\sin\left(\frac{QL}{2}\cos\alpha\right)}{\frac{QL}{2}\cos\alpha} \frac{J_1(QR\sin\alpha)}{QR\sin\alpha} + 2(\rho_{hydrophilic} - \rho_{solvent})V_{lipid} \times \frac{\sin\left(Q\left(\frac{L}{2}+t\right)\cos\alpha\right)}{Q\left(\frac{L}{2}+t\right)\cos\alpha} \frac{J_1(Q(R+t)\sin\alpha)}{Q(R+t)\sin\alpha} \quad (2)$$

where $J_1(x)$ is the first-order Bessel function of x, and α is the angle between the bilayer normal, **n**, and the scattering vector, **Q**, and V_i is the volume of species i in the disk. This model does not take into account interparticle interactions, resulting in a simplified formula for the scattering function, $I(Q) = \phi_{lp}P_{disk}(Q)$. Thus, only the scattering curve of the lowest c_{lp} in each series was fitted. During the fitting procedure, $\rho_{solvent}$ for D_2O was fixed to be 6.38×10^{-6} Å^{-2} and $\rho_{hydrophobic}$ was also calculated and fixed to be -4.3×10^{-7} Å^{-2}, based on the two hydrocarbon tails having a mass density of 0.85 g/cm^3. The thicknesses of the hydrophobic and hydrophilic layers, L and t, were constrained to be in the acceptable range of 20−40 Å for L and 5−10 Å for t.[16,17,26]

As shown in Figure 7, the fits are in excellent agreement with the SANS data. The structural parameters resulting from the fits are presented in Table 3 and are similar for both the PC and PC+PG series. This consistency il-

(26) Harroun, T. A.; Heller, W. T.; Weiss, T. M.; Yang, L.; Huang, H. W. *Biophys. J.* **1999**, *76*, 937. Harroun, T. A.; Heller, W. T.; Weiss, T. M.; Yang L.; Huang, H. W. *Biophys. J.* **1999**, *76*, 3176.

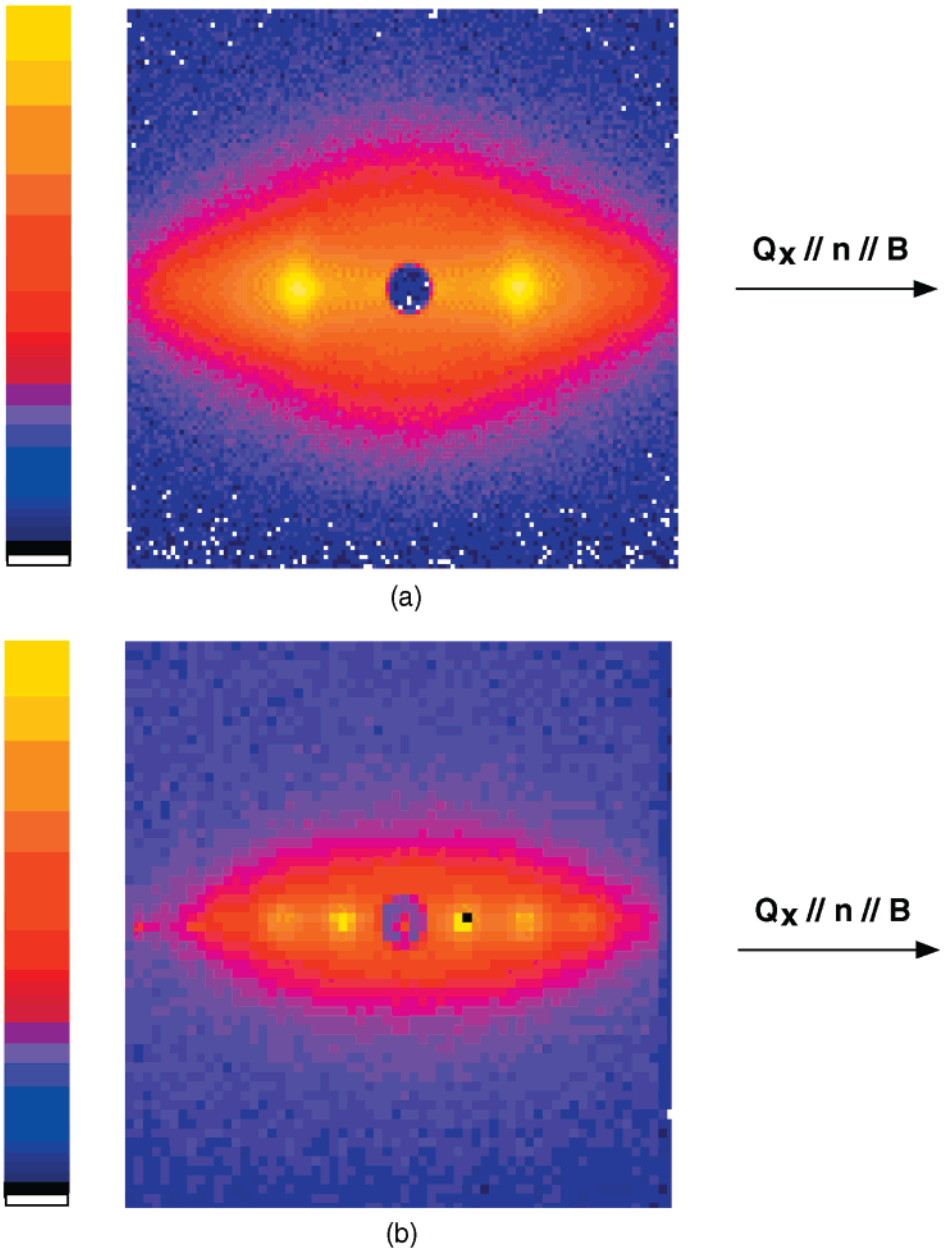

Figure 8. The 2-D SANS data for (a) PC+PG and (b) PC at $c_{lp} = 0.25$ g/mL at a sample-to-detector distance of 1.50 m in the presence of a 2 T magnetic field. The false color bars represent the scale of intensity from top to bottom. Bragg peaks appear in both (a) and (b) along **Q**, parallel to the **B** direction ($\mathbf{Q}_x$), indicative of $\mathbf{n}||\mathbf{B}$. The Tm^{3+} ion concentration in the PC series mixture in (b) was 10 times that of the PC+PG mixture in (a) and shows higher order diffraction peaks indicative of a more ordered structure.

lustrates that the addition of DMPG affected neither the structure nor the dimensions of the bicelles. The average t of the two systems is 7.5 ± 2.0 Å, as estimated in the literature.[16,17] The calculated value for $\rho_{hydrophilic}$ ($\sim$1.3 × 10^{-6} Å^{-2}) differs from the fitted $\rho_{hydrophilic} = (3.3 \pm 0.5) \times 10^{-6}$ Å^{-2} because of the inclusion of D_2O solvent in the hydrophilic headgroup region. Nevertheless, this fitted value for $\rho_{hydrophilic}$ is consistent with the value of 3.4 × 10^{-6} Å^{-2}, obtained from neutron reflectivity measurements by Meuse et al.[27] The fitted result of $d_{philic-philic} = L + t = 42 \pm 4$ Å was found to be about 7 Å larger than that in the high-T phase. This thickening is believed to be the result of a transition from the higher-temperature L_α phase, where the hydrocarbon chains are in a disordered molten state, to the lower-temperature L_β phase, where the chains are in a more ordered state with more of the hydrocarbon chains found in the all-trans configuration.[24]

In addition to the excellent agreement between the fits and experiment, further evidence for the bicellar phase is provided by the consistency of the best-fit parameters with the calculated ones. Using the assumption that the DHPC lipids occupy the edge of the bicelle and the DMPC lipids are on the major face of the bicelle disk, Vold and Prosser calculated R as a function of $(L + t)$ at a constant molar ratio of DMPC/DHPC as follows:[3]

$$\frac{[\mathrm{DMPC}]}{[\mathrm{DHPC}]} = \frac{2\pi R^2}{\pi(L + t)[\pi R + (L + t)]} \qquad (3)$$

The $(L + t)$ obtained from the fit is 42 ± 4 Å, resulting in $R = (210 \pm 20)$ Å at the DMPC/DHPC ratio of 3.2. This calculated R is also consistent with the fitted values of R,

(27) Meuse, C. W.; Krueger, S.; Majkrzak, C. F.; Dura, J. A.; Fu, J.; Connor, J. T.; Plant, A. L. *Biophys. J.* **1998**, *74*, 1388.

which are (196 ± 20) and (189 ± 20) Å for the PC and PC+PG series, respectively.

B. Data in a Magnetic Field. It is well-known that the Tm^{3+}-doped bilayered system cannot be aligned under the influence of a magnetic field at temperatures below 35 °C. However, at temperatures above 35 °C and for 0.05 g/mL < c_{lp} < 0.25 g/mL, the doped system can be aligned with the bilayer normal parallel to the field, that is, **n**||**B**. We conducted out-of-plane (**Q**||**n**) and in-plane (**Q**⊥**n**) scattering experiments on both PC and PC+PG series samples with a c_{lp} of 0.25 g/mL at 45 °C. As the incident beam was defined to be along the *z*-axis and thus the detector was in the *x*−*y* plane, the out-of-plane scattering was measured in a horizontal magnetic field, along *x*, that is, $\mathbf{Q}_x$||**B**||**n**. When the magnetic field was turned off, the degree of alignment was retained for several hours. Hence, for the in-plane scattering measurements the sample was aligned in the magnetic field, then the field was turned off, and the sample was rotated 90° such that **Q**⊥**n** for all directions on the area detector (i.e., **n**||**z**).

In the applied field, at 45 °C and c_{lp} = 0.25 g/mL, the scattering pattern transformed from a typical "powder" pattern to the out-of-plane scattering indicative of an aligned system (Figure 8), as expected.[9−11] Our SANS results for both series confirm that **n** is parallel to **B** for these low-Tm^{3+}-doped systems. Although only low concentrations of Tm^{3+} (Tm^{3+}/DMPC = 0.0065) are needed to align the bilayers,[10] only the first-order diffraction peak was observed in our experiments for both the PC+PG series (Figure 8a) and PC (data not shown). A comparison experiment was conducted using a PC series sample doped with 10 times more Tm^{3+} ions. Higher order scattering peaks indicative of a more regular spacing in ξ_D (Figure 8b) were observed in this case, consistent with a previous neutron diffraction result, which recorded five Bragg peaks.[9]

For PC mixtures of low Tm^{3+} concentration, the invariance of the scattering peak position, seen in Figure 9a for the different scattering geometries, that is, **Q**||**n**, **Q**⊥**n**, and randomly oriented lamellae, implies that the alignment of the bilayers, rather than their intrinsic structure, is affected by the presence of the magnetic field. A residual peak seen in Figure 9a for the in-plane scattering from the PC samples indicates that a portion of the lamellae did not align with **n**||**B**. No residual peak was observed in the PC+PG mixture (Figure 9b), suggesting that the inclusion of lipid salts increased the alignment of the system in the applied magnetic field. This is consistent with the NMR results of Struppe et al.[8]

Assuming the bilayers were well aligned in the magnetic field for the PC+PG series, one can obtain more detailed information about the bilayer surface structure from the in-plane scattering. We attempted to model this scattering as coming from disklike perforations (pores) in the aligned bilayer sheets. Therefore, to specify the pore alignment we used eq 2 for $P_{pore}(Q)$, the form factor of the pores, and set $\alpha = \pi/2$. The radius of the pores was assumed to follow the Schulz distribution function. While determining the radius of the pores through fitting, the values of all the SLDs and the bilayer thickness were fixed according to the previous fitting results in Tables 2 and 3. The best-fit curve (the solid line) in Figure 9b, corresponding to R = 18 ± 3 Å and a polydispersity of 0.35 ± 0.05, shows good agreement with the data in the range of $Q > 0.02$ Å^{-1}. The excess scattering at $Q < 0.02$ Å^{-1} is also present in the data in zero field (Figure 1b) and may indicate the presence of some larger scale in-plane inhomogeneities.

The fitted result for the volume fraction of these "pores", ϕ_{pore}, is 0.18 ± 0.03. The total volume fraction occupied by the bilayers can be approximated by ($\phi_{lp} + \phi_{pore}$), resulting in the value of 0.41, which is relatively close to ϕ_{calc} for the PC series in Table 1, implying that the perforated structures on the bilayers of PC and PC+PG are similar to each other. Nevertheless, ($\phi_{lp} + \phi_{pore}$) remains smaller than ϕ_{calc} for the PC+PG series possibly because of the nonuniform dispersion of the lipids in solution as mentioned previously.

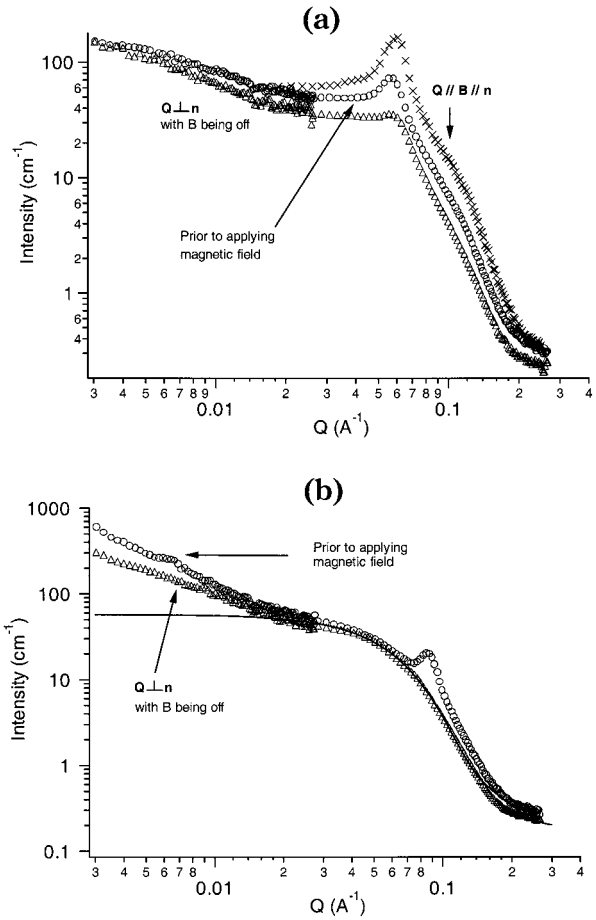

Figure 9. Comparison of the scattering, in the aligned and randomly oriented states, from both series mixtures at 45 °C and c_{lp} of 0.25 g/mL. (a) Shown for the PC series is the out-of-plane ($\mathbf{Q}_x$||**B**||**n**), randomly oriented, and in-plane (**Q**⊥**n**) scattering. (b) The PC+PG series includes the randomly oriented and in-plane scattering. The solid curve in (b) shows the best-fit result for the perforations in the bilayers, modeled as "disks" in the bilayer plane.

Discussion

I. Perforated Lamellar Phase (High *T* and High c_{lp}). The scattering curves of the PC and the PC+PG series (Figure 1a,b) are qualitatively the same, indicating that the addition of DMPG does not alter the basic morphology of the reference system, consistent with other literature reports.[8,10,13] Some indication of the rigidity of the bilayers can also be obtained from the ϕ_{lp} dependence of the scattering. Strey et al. derived an expression for determining the membrane rigidity, K, in terms of c_{lp}, ξ_D, and bilayer thickness $t_{bilayer}$ as follows:[28]

$$\phi_{lp}\xi_D = t_{bilayer}\left[A - \frac{k_B T}{4\pi K}\ln(\phi_{lp})\right] \qquad (4)$$

(28) Strey, R.; Schomacker, R.; Roux, D.; Nallet, F.; Olsson, U. *J. Chem. Soc., Faraday Trans.* **1990**, *86*, 1690.

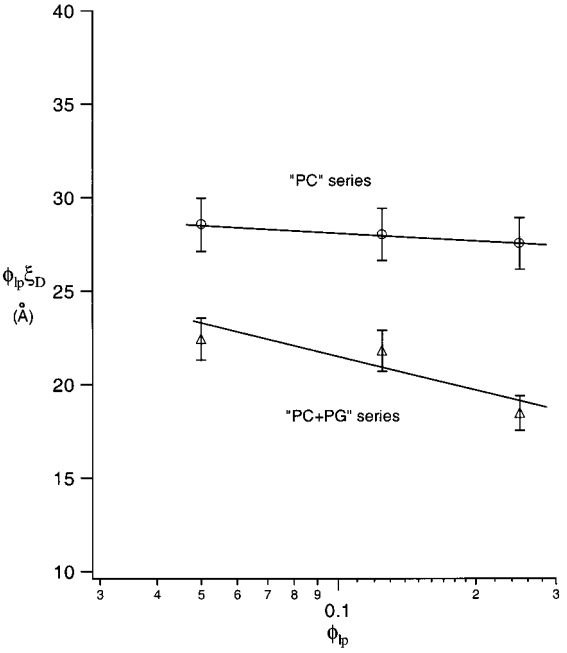

Figure 10. The product, $\phi_{lp}\xi_D$, of the known total lipid volume fraction in each sample, ϕ_{lp}, and the interlamellar spacing, ξ_D, as a function of $\ln(\phi_{lp,act})$. The circles (○) and triangles (Δ) are for PC and PC+PG, respectively. According to eq 4, the slope is inversely proportional to the bilayer rigidity, K. From the linear least-squares fits, the slope was found to be −0.6 for PC mixtures and −2.4 for PC+PG mixtures. Thus, K is larger for the PC series, implying that the PC bilayers are more rigid than the PC+PG bilayers.

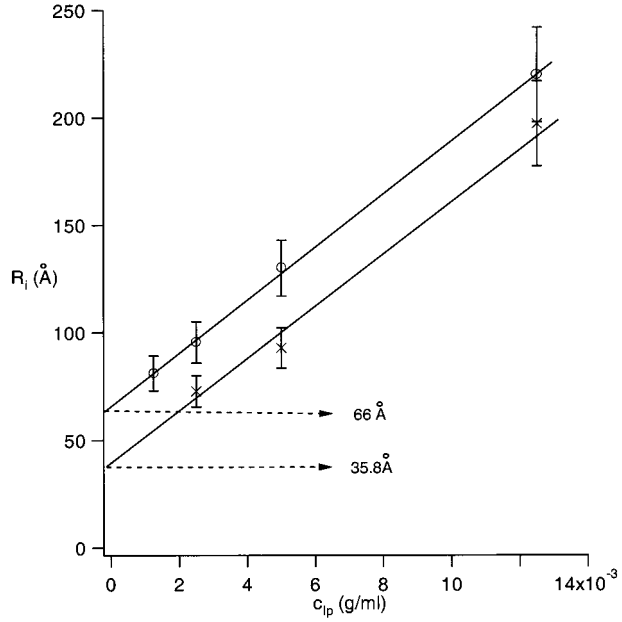

Figure 11. The relationship between R_i, the inner radius of the unilamellar vesicles, and c_{lp}, the known total lipid concentration. The circle (○) and cross (×) symbols represent the PC and PC+PG series mixtures, respectively. By extrapolation to $c_{lp} = 0$, the infinite dilute R_i is 66 Å for the PC series and 35.8 Å for the PC+PG series.

where A is a constant, k_B is the Boltzmann constant, and T is the temperature. The ϕ_{lp}-dependent term at the right-hand side of eq 4 is attributed to the "excess area" of the lamellae, which is defined as the ratio of the actual surface area to its projected area perpendicular to the average bilayer normal, minus 1.[18,28] For rigid lamellae, $K \rightarrow \infty$ so $k_BT/4\pi K \rightarrow 0$. On the contrary, the more flexible the lamellae (the smaller the value of K), the larger is the absolute value of this term. The product of ϕ_{lp} and ξ_D plotted as a function of $\ln(\phi_{lp})$ is linear with a slope proportional to $-1/K$. Figure 10 shows that the PC series bilayers are more rigid (5.0 k_BT) than those in the PC+PG series (1.3 k_BT). This difference is related to the charge density on the lamellae.[29] For the PC+PG series, a smaller charge density on the lamellae than in the PC series because of charge compensation results in more flexible bilayers.

II. Unilamellar Vesicular Phase (High *T* and Low c_{lp}). For the vesicular phase, Oberdisse and Porte have systematically studied the influences of both lipid and salt concentrations as well as the bilayer charge density on the radius of single vesicles in dilute solutions.[30] Our experimental results are consistent with theirs in that R_i (or R_o) decreases with decreasing lipid and salt concentrations and with increasing bilayer intrinsic charge (through the addition of DMPG). By extrapolating the regression lines to $c_{lp} = 0$ in Figure 11, R_i in the infinite dilute salt and lipid solution can be deduced to be 66 Å for PC vesicles and 35.8 Å for PC+PG vesicles. The polydispersity of the vesicular radius, p, was almost independent of c_{lp} except that a higher p was obtained at $c_{lp} = 0.0125$ g/mL, possibly because of the residual lamellae in the system. Note that at the two highest c_{lp} (0.0125 and 0.005 g/mL) in the vesicular phase, the $\phi_{lp,fit}$ is greater than the experimental prepared ϕ_{lp}. This may be due to perforations on the vesicular surface. Nevertheless, at lower c_{lp} ($c_{lp} < 0.0025$ g/mL) the $\phi_{lp,fit}$ agrees with ϕ_{lp}, indicating no significant porosity on the vesicles.

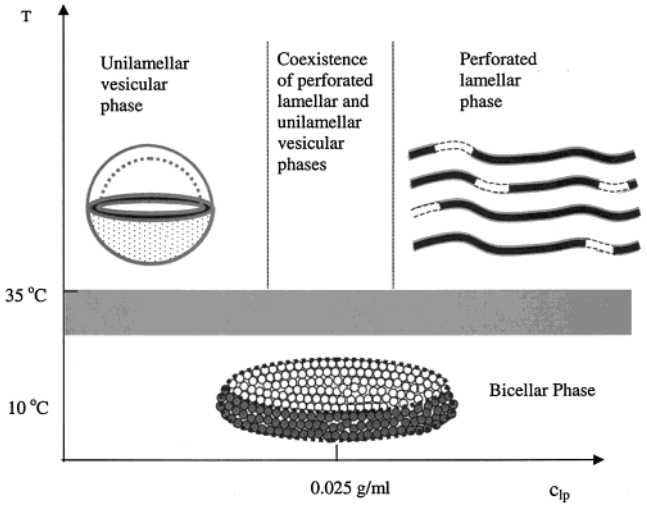

Figure 12. The phase diagram deduced for the PC and PC+PG series mixtures. Three phases are depicted (detailed explanation in text). The phase-transition temperature, 35 °C, is obtained from NMR study[11] but was not well established in this study. The phase-transition $c_{lp} = 0.025$ g/mL at high temperature was obtained from our dilution measurements.

III. Phase Diagram. Summarizing our results, we can construct a phase diagram as a function of T and c_{lp} for both the PC and PC+PG series of mixtures (Figure 12). Because measurements were taken at only two temperatures (10 and 45 °C), the well-defined phase-transition boundaries for T and c_{lp} are not available. At 10 °C, only one phase, the bicelle, is found in the range of c_{lp} studied. The temperature-induced phase transitions are bicelle to perforated lamellae at high c_{lp} values (0.05 g/mL < c_{lp} < 0.25 g/mL) and bicelle to vesicle at low c_{lp} (<0.05 g/mL).

(29) Higgs, P. G.; Joanny, J.-F. *J. Phys.* (*Paris*) **1990**, *50*, 2307.
(30) Oberdisse, J.; Porte, G. *Phys. Rev. E* **1997**, *56*, 1965. Oberdisse, J. *Eur. Phys. J. B* **1998**, *3*, 463.

The phase boundary at 35 °C was chosen from the NMR studies[11] and the onset of a dramatic change in viscosity. As c_{lp} increases at a constant high temperature (45 °C), the vesicular radius increases to the point that the large vesicles (R_o > 260 Å) become unstable and the system gradually transforms into the perforated lamellar phase with a coexistence region at ∼0.025 g/mL, as mentioned previously.

Conclusions

Using SANS, we have successfully determined the morphologies formed by the mixtures of DMPC/DHPC and DMPC/DHPC/DMPG bilayers doped with Tm^{3+} ions over a wide range of temperatures and lipid concentrations. Our results indicate the following:

(a) For both lipid mixtures at high lipid concentrations and an elevated temperature (45 °C), we have obtained scattering patterns that are consistent with stacks of perforated lamellae. This morphology is consistent with the "Swiss cheese" structure proposed by Prosser et al.[11]

(b) At a temperature of 45 °C and c_{lp} < 0.025 g/mL, a unilamellar vesicle phase was discovered. It was observed that the radius of the vesicles decreased linearly with decreased c_{lp}, and the bilayer thickness was found to be the same as that determined in the perforated lamellar phase. Also, in the c_{lp} range between 0.005 and 0.0125 g/mL, the perforated lamellar structure may persist into the vesicular phase. As c_{lp} was further decreased, the perforated lamellar structure became insignificant.

(c) At a temperature of 10 °C, only one phase, namely, the discoidal bicelle, was observed throughout a wide range of c_{lp} (0.25 g/mL ≥ c_{lp} ≥ 0.00125 g/mL). A significant difference between the perforated lamellar phase (or unilamellar vesicular phase) and the discoidal bicelles is the change in the bilayer thickness, which increases by ∼7 Å as the phase transforms from the perforated lamellar phase (or unilamellar vesicular phase) to the bicelle morphology. This is indicative of more ordering of the hydrocarbon chains.

(d) Addition of the charged lipid DMPG did not perturb either the basic morphology or the orientation of the lipid but resulted in the alteration of various structural dimensions including ξ_D. Our data also illustrated that the introduction of DMPG might result in the formation of lipid-rich domains.

(e) In magnetic alignment experiments, Tm^{3+} plays an important role in aligning the lamellar phase. Although the lamellae can be oriented with $\mathbf{n}||\mathbf{B}$ using minimal amounts of Tm^{3+} ions, ξ_D, as judged by the absence of higher order scattering peaks, was less regularly spaced compared with the sample containing 10 times greater amounts of Tm^{3+} ions.

LA001567W